Title:

Surface roughness assessment on hole drilled through the identification and clustering of relevant external and internal signal statistical features

Authors:

Aitor Duo[1,2](aduo@mondragon.edu), Rosa Basagoiti[1], Pedro J. Arrazola[2], Mikel Cuesta[2], Miren Illarramendi[1]

Affiliations:

[1]Data analysis and cybersecurity research group, Mondragon Unibertsitatea, Loramendi, 4; 20500 Arrasate-Mondragon (Gipuzkoa), Spain

[2]High-performance machining research group, Mondragon Unibertsitatea, Loramendi, 4; 20500 Arrasate-Mondragon (Gipuzkoa), Spain

Abstract

Drilling is a continuous cutting process where two or more cutting edges remove the material, to obtain the desired feature. During the chip evacuation, it generally rubs against the generated surface. Thus, the roughness obtained differs from other machining processes such as turning or milling. Therefore, surface roughness can be different from the analytically expected one. In this research work, an analysis of the cutting conditions where a level of roughness is expected to meet specific requirements has been carried out. 600 holes were made with two different tool geometries on steel without modifying the cutting conditions. When analysing the surface generated, certain variability in the roughness profiles obtained can be observed. External signals to the machine tool were acquired with sensors (cutting forces, vibrations, and acoustic emissions) as well as internal signals (spindle power, spindle torque in the Z-axis, spindle current and positions, speeds, accelerations, and jerk of the tool tip in the three axes of the machine). The most representative statistical features of the signals regarding roughness were selected using correlation analysis. Besides that, the hierarchical clustering of statistical features of the external and internal signals of the process was compared with clusters obtained using roughness parameters. Results show that clusters appear using signals highly related to the roughness parameters obtained from the measured profiles, confirming a mapping between the acquired signals during the machining process and the roughness of the holes.

1 Introduction

The control and monitoring of machining processes is an area of research with years of experience with increasing decision-making achievements. The most studied problem is tool wear [1–5], which, given the variability in the different operations involved in machining, can be manifested in different signals such as cutting forces [6,7], vibrations [8,9], acoustic emissions [10,11] or spindle power [12,13]. The tool condition can have a remarkable influence on surface integrity and thus, in component life. Generally, the surface integrity (surface roughness, residual stresses, or material damage) is linked to the tool condition, and the use of virtual metrology which can achieve real-time and complete on-line inspection can be of great help in terms of saving time and resources, as well as for decision making. The increase in demand for components with more precise finishes means that quality inspection of machined parts is becoming more critical and must be carried out with greater precision. This is a challenge for repetitive parts that must meet certain requirements, but for small batches production of high benefit components as well. Decisions regarding critical events that may

occur during a process should be made as quickly as possible. The automation tasks for the quality control of components acquire a significant role since they increase the production of components demanding some given requirements.[14]

Drilling is a cutting process where one, two or three cutting edges remove the desired material volume to produce a hole. The material removal in drilling is continuous, but the drill bit is confined inside the feature generated during the process. In this process, although most of the material is removed by the major cutting edges, it is the minor cutting edge that generate the desired surface. Thus, some problems are present, (i) the amount of heat going to the cutting tool is higher than other machining processes as the proper cooling of cutting edges is more complex, (ii) the surface roughness generated by the drill is modified by the chip generated and more complicated to be measured. However, hole making is usually performed, followed by the component finishing operations, in the final stages of the whole machining process chain of the component process and thus an error can produce a scrap component. Thus, systems that allow the interpretation and classification of the generated surface could help obtain a more robust production of components.

Surface roughness is a widely used indicator of technical requirements of a component [15]. The parameters that can be obtained from the surface roughness profile are shown in Table 1. These parameters are explained in detail by Gadelmawla et al. [16].

Table 1 *Roughness parameters from the profile measured on the surface of the component (ISO 4287-1997* [17]*)*

Name	Description	Unit
Ra	Average roughness of profile	µm
Rq	Root-Mean-Square roughness of profile	µm
Rt	Maximum peak to valley height of roughness profile	µm
Rz	Mean peak to valley height of roughness profile	µm
Rmax	Maximum peak to valley height of roughness profile within a sampling length	µm
Rp	Maximum peak height of roughness profile	µm
Rv	Maximum valley height of roughness profile	µm
Rc	Mean height of profile irregularities of roughness profile	µm
Rsm	Mean spacing of profile irregularities of roughness profile	µm
Rsk	Skewness of roughness profile	
Rku	Kurtosis of roughness profile	
Rdq	Root-Mean-Square slope of roughness profile	
Rt/Rz	Extreme Scratch/Peak value of roughness profile, (>=1), higher values represent larger scratches/peaks	

Among all these parameters, the most used one is *Ra*. However, this parameter alone does not explain the entire roughness profile for the machining process. Fig 1 a) shows two different roughness profiles with the same *Ra* and different skewness, Fig 1 b) shows two different roughness profiles with the same *Ra* and different kurtosis. Most of the standard machining processes produce surfaces with asymmetric (non-Gaussian) profiles. Turning and shaping generate rough surfaces with positive skewness. Whereas grinding, honing and milling generate rough surfaces negative skewness and high kurtosis, surface with negative skewness always has a larger contact area ratio [18]. Wern et al. [17] show that this process generates a negative skewness and a high kurtosis in the case of drilling processes. Amor et al. [19] showed that profiles with the same level of roughness *Ra* and different degree of skewness -*Rsk*- do not have the same contact properties. They also showed that the negative skewness and the lower value of *Ra* are advisable to achieve a high normal contact stiffness. The profile with positive skewness shows a smaller support area. However, the negative skewness profile can lead to

fracture propagation and therefore, can have a negative effect on the fatigue life of a component. Thus, it is important to consider more than one parameter among those obtained from the roughness profile to have a clear reference of the requirements to be fulfilled by the machined component.
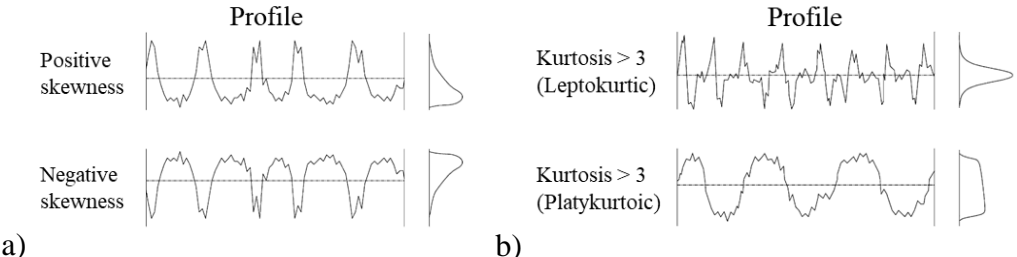

Fig 1 Surface roughness profiles with same Ra parameter a) different skewness distributions b) different kurtosis distributions. (extracted from [20] [16])

From the list of roughness parameters shown in table 1, *Rt, Rmax, Rp* and *Rv* take into account a single value of the whole measured roughness profile. On the other hand, *Ra, Rq, Rz, Rc, Rsm, Rsk, Rku* are more descriptive values of the roughness distribution. *Rdq* is the only hybrid parameter. This parameter can be obtained by calculating all the slopes between every two successive points of the profile and calculating the average of these slopes. Mechanical properties such as friction, elastic contact, reflectance, fatigue crack initiation and hydrodynamic lubrication affect this parameter [20].

The dominant process parameter is the feed rate. In the literature, the increase in feed rate is related to increased roughness due to increased feed marks or plastic deformation because of the load on the cutting edge [21,22]. Fig 2 shows the drilling process and the generated surface. At each spindle revolution, each cutting edge removes half of the material programmed for the feed per revolution. Tool wear may be one of the causes for the generated surface to be affected, although there is no direct relationship between these two parameters. The diameter is slightly reduced towards the shank end of the drill bit, which is known as "back taper", which prevents friction and heat (represented as the β angle). The review made by Thakur et al. [23] shows cases where the roughness is better even with a worn tool explaining this phenomenon by the displacement of the trailing edge, which acts as a cleaner to reduce the peaks of the generated surface in turning processes. However, this is only valid in cases where the flank wear is uniform. Other types of tool wear, such as chipping of the cutting edge, adhesion or attrition, cause a worsening of surface roughness.
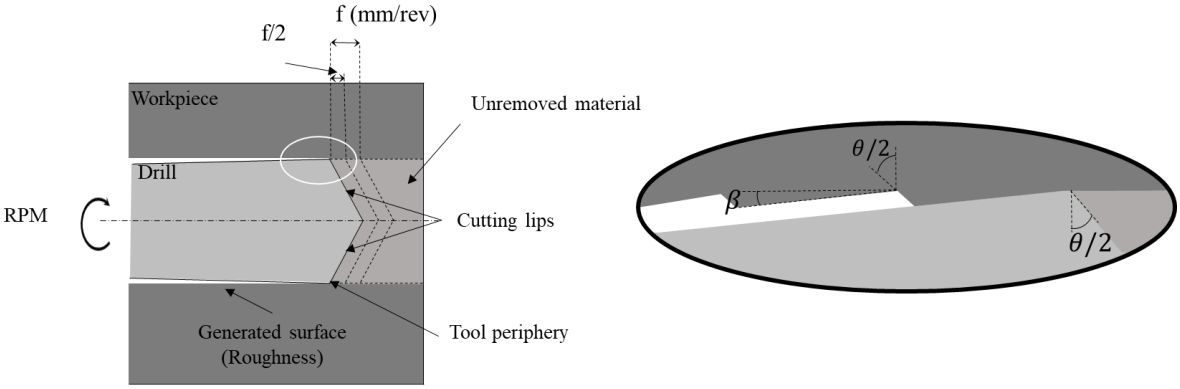

Fig 2 Drilling process and the generated surface where θ is the point angle and β represents the difference between the body clearance diameter and drill diameter called back taper

Regarding surface finish monitoring systems, Garcia Plaza et al. showed various advanced signal processing techniques for surface roughness prediction in turning process. such as signal spectrum analysis employing vibration signals [24] Wavelet packet transform employing cutting force signals [25] and compared also non-advanced signal processing methods and advanced signal processing methods on vibration signal [26], showing the superiority of the second one. On these works they used 270 roughness measurements for training and 90 roughness measurements for testing the multivariate regression models. Akincioğlu et al. [27] were conducting a study on steel to predict the *Ra* parameter. They used different cutting conditions for each hole they make, so they do not consider the phenomena that could appear during the drilling of holes under established cutting conditions. 32 holes were drilled, 26 were used for the learning phase and 6 for the testing phase obtaining RMSE= 0.010594.

Most of these works consulted in the literature are based on supervised learning. Furthermore, most works used as learning data the cutting conditions used, assuming that the same roughness will always be obtained at specific cutting conditions. The use of signals external (Cutting forces, vibrations, or acoustic emissions) or internal (Spindle power or current) to the machine could deal with the classification of roughness. However, the systematic measurement of the roughness of a component could be a problem since it is time expensive. Most works are based on changing the cutting conditions, but few repetitions are made with each condition, not achieving a good generalisation. In extended machining time, the probability of an undesirable phenomenon and a resulting defective component is high. These are still a low number of observations for implementing a real roughness monitoring system based on machine learning supervised classification algorithms. This low number of observations shows the difficulty in measuring and preparing data for a monitoring system of the roughness in drilling processes. Besides that, the mentioned works did not consider various roughness parameters such as *Rsk* or *Rku,* which explain the non-Gaussian nature of a roughness profile. Roughness characterisation based on additional parameters can give more information, and a model can show a greater generalisation of the obtained data. Regarding signals, both external and internal process signals contain information about the transient and non-transient events of the cutting process. Therefore, methodologies that help to understand and extract information from these signals can help to speed up the process of building models that allow the prediction of the roughness of a machining process.

From another perspective, most of the work observed focuses on supervised learning. This implies the measurement and extraction of the variables to be monitored before the learning phase. On the other hand, clustering is an unsupervised method that allows the understanding of groups and improves the knowledge about the process, dealing with unlabelled data and trying to explain groups created from this data. The clustering algorithm groups the observations in subsets of data, and similar observations are grouped, while observations with differences belong to different groups. Clustering methods organise the observations into an efficient representation that characterises the target population of the sample [28]. Unsupervised methods can be divided into two groups, hierarchical or partitioning methods. Hierarchical methods, build the groups by dividing the observations recursively. The result is a dendrogram representing the groupings of observations and their level of similarity. Partitioning methods create an initial partition and reallocate observations from one group to another. These methods usually require the number of groups to be selected previously. The hierarchical methods are divided into two groups, agglomerative methods, which consider each of the observations as an independent cluster and group them and divisive methods, which consider the whole set of observations as a cluster and separate them into subgroups. Among the agglomerative methods, different inter-group proximity measures may show more or less

interpretable results in the same group of observations In [29] hierarchical clustering methods can be consulted.

PCA allows to reduce a big feature space d into lower feature space k, where $k < d$, preserving the original d dimensional space information. Each k dimensions will be transformed as linear combinations of d dimensional feature space. This allows the identification of the dominant features from the original d dimensional space as well as a more analytical visualization of the results. A more detailed explanation of this method can be found on [30].

Mingoti and Lima [31] compared different partitioning and hierarchical clustering algorithms, SOM (Self Organizing Map) networks, Fuzzy c-mean, K-means and hierarchical agglomerative clustering on simulated overlapped data and with outliers. In the study, they showed that Fuzzy c-means behaves well concerning the other partitioning algorithms. Regarding hierarchical agglomerative algorithm, among the different measures used of inter-group proximity, they showed that the Ward method is the one that obtains the most stable behaviour. Diaz-Rozo et al. [32] used both hierarchical and partitioning clustering algorithms to diagnose the state of a spindle. Xiaoli and Zhejun [33] used fuzzy partitioning algorithms to classify different levels of tool wear in boring operations. Partitional Around Medoids (PAM) algorithm was used by Li et al. [34] for tool wear state clustering in milling operations showing its superiority over k means and fuzzy c means algorithms based on cutting force signal. Zhou et al. [35] used vibration signal time-frequency features and fuzzy c means algorithm to classify 3 roughness Ra ranges in the drilling operation. Kubišová et al. [36] used hierarchical clustering to compare original surface roughness with replicated surface roughness based on Euclidean distances of various roughness parameters showing that it can be a good tool for replicability measurements of obtained surface profiles.

To sum up, the different methods used for interpretation of results based on unsupervised learning have not been widely used for monitoring purposes in the field of machining. These methods allow the extraction of knowledge and accelerate decision making without the systematic measurement of interest parameters in the industry. Regarding the roughness obtained, it is necessary to interpret the distribution of the data obtained from the surface for a better interpretation and compliance with the requirements depending on each sector. The comparison of similarity between the different roughness parameters and the statistical features extracted from the signals can lead to the interpretation of surfaces and the variation between them.

In this paper, the authors study hierarchical clustering methods to obtain indicators that approximate the measured roughness distributions. The methodology followed in this analysis is, first, to obtain the statistical features of the internal and external signals that are related to roughness parameters obtained in the Alicona profilometer for some of the samples. Then, a clustering of the measured roughness parameters is performed using many parameters extracted from the roughness profile. By means of a correlation analysis between statistical features of the acquired signals and the obtained roughness parameters, those signals that maintain a high linear correlation are identified. Once the relevant parameters are identified, a clustering is carried out in a wider space of observations.

In the following sections, the experimental set-up is first presented. Then, the feature extraction method used is showed and how a suitable feature subset was selected. After that, the clustering results for hole surface properties assessment are shown. Finally, the concluding remarks are presented.
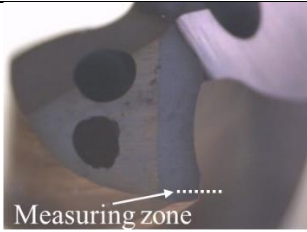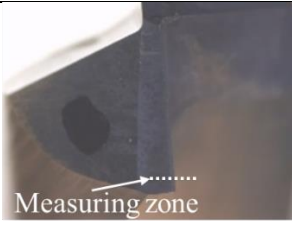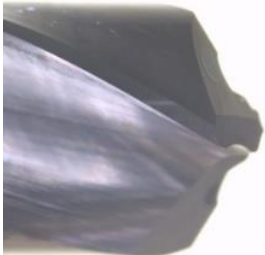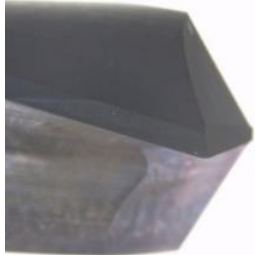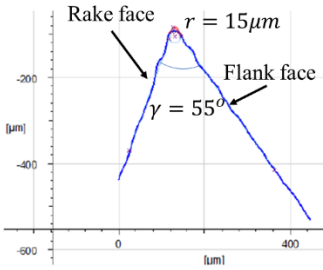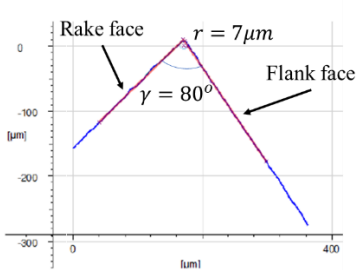
2   Methodology

This section explains the work carried out for the determination of roughness obtained during drilling processes using internal signals and sensor data. Specifically, the experimental set-up used, the roughness measurements obtained from each of the holes and projections using PCA after the groups identified with different roughness levels by the hierarchical clustering algorithm.

2.1   Experimental set-up

The tests were carried out on a Lagun vertical milling machine tool. Two different tool geometries were used (R204.6D and BH04.5D), and a total of 600 holes were produced with each tool, the tool geometry and the cutting conditions used with each of them can be observed in Table 2. The cutting edge radius and the wedge angle were measured at the periphery of the tool before starting the tests. During the tests, the tool was inspected on the lip and outer corner of the point with a frequency of 20 holes in a Leica DMS1000 macroscope with no evidence of tool wear. The workpiece material was a 35CrMo4 steel.

Table 2 Tool geometries and cutting conditions used during the tests

Drill type	R204.6D	BH04.5D
Cutting edge		
Drill periphery		
Drill geometry		
	Helix angle = 30º	Helix angle = 15º
	Coating = TiAlN	Coating = TiAlN
	Cutting edge radious (r)= 15µm	Cutting edge radious (r)= 7µm
	Wedge angle (γ)= 55º	Wedge angle (γ)= 80º
	Point angle = 140º	Point angle = 140º
Cutting conditions	Vc=100 m/min; 3978 RPM	Vc=70 m/min; 2785 RPM
	f=0.15 mm/rev	f=0.15 mm/rev
	Ø=8 mm	Ø=8 mm
	Through hole depth=5 mm	Through hole depth=5 mm
	Coolant = None	Coolant = None

A Kistler 8152C acoustic emission sensor with a Sampling Frequency (Fs) of 1 MHz, a PCB J356A45 triaxial accelerometer with a Fs=25.6 kHz and a Kistler 9123 4-component rotational dynamometer with a Fs of 10 kHz were installed for signal acquisition. Besides, several internal CNC signals were collected at 250 Hz sampling frequency, concretely: TV2 (Z-axis motor torque), TV50 (spindle motor power feedback), TV51 (active power supplied by the drive) and TV3 (power percentage used with respect to the maximum power available in the servo system. The tool tip position and its derivatives (tool tip speed, acceleration and jerk) where acquired in the three axes together with the spindle speed and feed rate. The acquisitions were made for every 5 holes.

For the simultaneous acquisition of the signals, the threshold (PFI0) was configured in the acquisition cards so that when the internal acquisition started, the external signals would start to be collected simultaneously. An analogue output (ao0 of the CNC) of the machine tool was used to obtain a threshold at the time of the acquisition, and this allows to obtain both internal and external signals simultaneously. The surface of the workpiece is Z=0 mm, when the position of the tool tip is Z=1 mm, the command is given to start the simultaneous acquisition on the NI USB 6361 and NI cDAQ 9178 acquisition cards. The experimental set-up and acquisition system used can be seen in Fig. 3. The internal signals of the machine were acquired at the CNC itself while the external signals were acquired in an external PC.
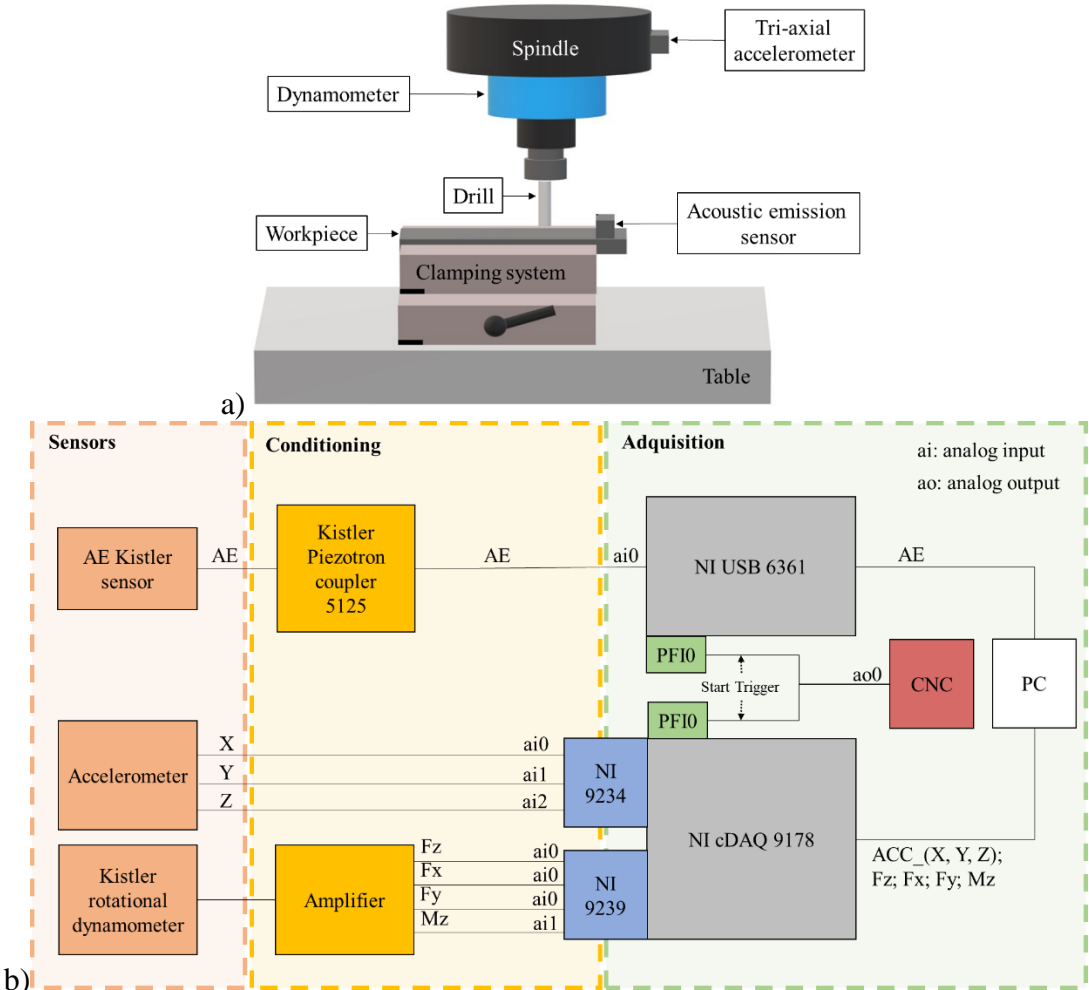

Fig 3 *a) Experimental set-up and b) acquisition system*

2.2 Surface roughness measurements

After the tests, 6 holes were cut and measured in the Alicona profilometer per each of the tools used to observe variability in the roughness level obtained. These holes were selected at random, scattered over time. From the holes made with the straight-edge tool (BH04.5D), holes 181, 182, 183, 287, 381 and 581 were selected. From the holes made with the curved-edge tool (R204.6D), holes 45, 196, 306, 310, 411 and 521 were cut.

All these holes have been cut from the middle in two parts, each of these parts has been measured by a cross-section, obtaining two measurements for each of the holes. Each of the measurements is 7.16 ° of the hole perimeter. There is an example of the measurement of the holes in Fig. 4.
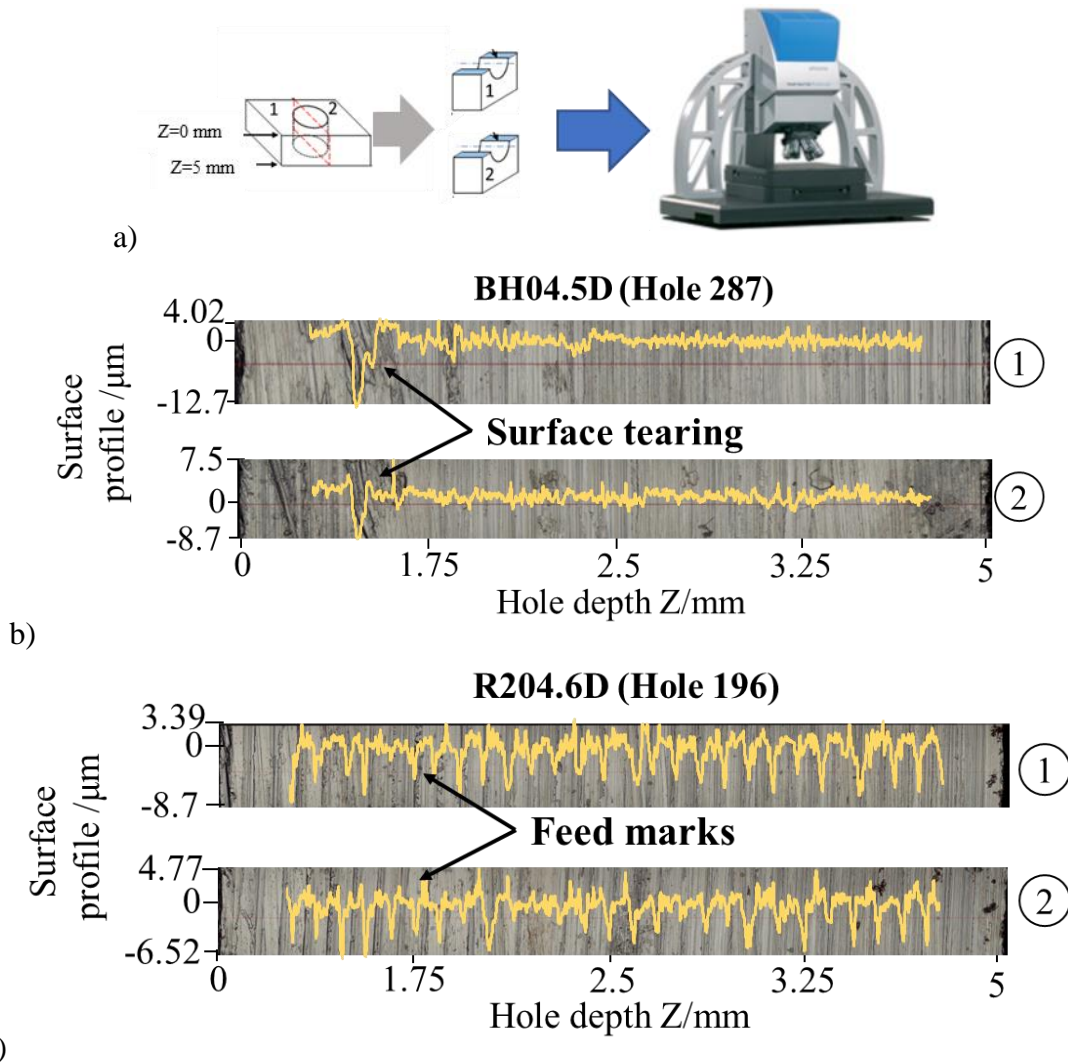

Fig 4 Example of Alicona measurements for hole 196 of curved edge tool and hole 287 for straight edge tool a) Hole cutting and measurement process b) 1st and 2nd measurement of hole number 287 made with BH04.5D tool c) 1st and 2nd measurement of hole number 196 made with R204.6D tool
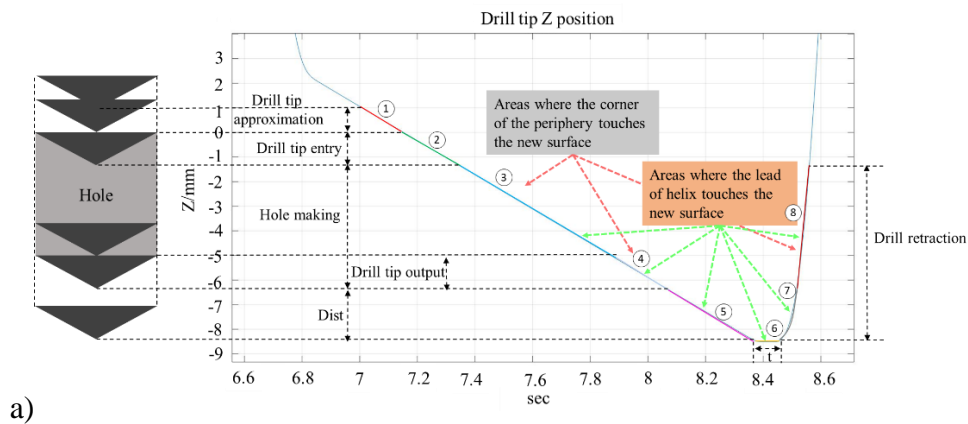
All the parameters shown in Table 1 were obtained for every measurement made, even though many of these parameters are highly correlated and do not provide extra information. However, the use of only the *Ra* measurement for the characterisation of the roughness quality of a surface was not sufficient. A selection process was carried out that adequately described the generated surface and will be explained in section 2.3.

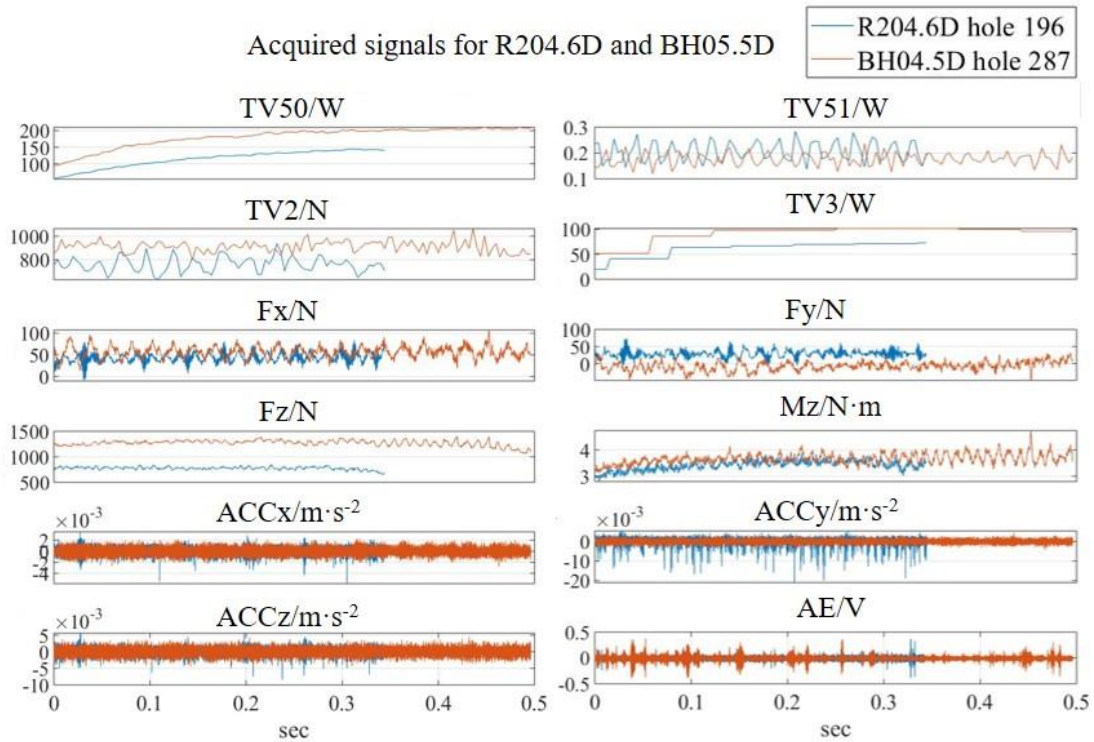## 2.3 Acquired signal segmentation and feature extraction

Regarding the acquired external and internal signals, different drilling process phases were identified, depending on the tool tip position of the drilling process, as shown in Fig 5 a). Within these phases, signals are most stable in phase 3. In phase 2, the tool begins to penetrate the material until the height of the drill tip is entirely within the material. In phase 4, the tool tip starts to emerge from the bottom of the workpiece material and the signals start to attenuate by the loss of contact between the tool and the workpiece. Once in phase 5, the tool descends to a point where the burr is minimised outside the hole. Depending on how the drilling cycle has been programmed, phase 6 keeps the tool at the lowest point for a while. During the retraction of the tool, two phases have been considered, phase 7, that corresponds to the tool path where the periphery of the tool tip is below the working material and phase 8, which corresponds to the path taken by the tool as long as the periphery of the tool tip is completely out of the drilled hole.

Changing the spindle RPM affects the sampling frequency of the acquired signals. Taking the sampling frequency of the cutting forces as a reference (10kHz) with the R204.6D tool at a speed of 3978 rpm, the sampling frequency per revolution was 150 samples/rev. While with the BH04.5D tool at a speed of 2785 rpm, 215 samples/rev. This means that with the R204.6D tool 30% less data is acquired than with the BH04.5D tool.

The signals acquired have been segmented, and only the part belonging to phase 3 (Hole making) of the drilling of a hole has been retained. Specifically, the signals have been segmented from the moment the periphery of the tool tip is entirely inside the material until the tool tip starts emerging from the bottom of the material. Fig 5 b) is an example of the different signals acquired for phase 3.

a)

Fig 5 Segmented signals a) Tool tip position and each drilling stage b) Acquired signals of the third stage of the drilling process for both tool geometries

As part of the first stage, and to eliminate some noise introduced by the machine in the vibration signals, signals have been filtered with a low pass Butterworth filter of order 10 with cut-off frequency Fc=3600 Hz and a bandpass filter with Fc1=4000 Hz and Fc2=6000 Hz, using these signals separately. On the one hand, we have the vibrations that happen below 3600 Hz (named ACC(x-y-z)_1) and in the other hand, vibrations in the sub-band 4000-6000 Hz (named ACC(x-y-z)_2). Six vibration signals overall, two for each signal acquired on each of the three axes.

These 15 signals are available for the clustering of the holes and after extracting eight statistical features for each one, *mean, rms, standard deviation, maximum, minimum, kurtosis, skewness and variance*, 120 statistical features are finally available. In a previous work [14], the authors, using the same features, analysed the linear relationships between internal and external signals.

The workpiece features (roughness measurements) and sensor signals were obtained from the drilling process to be related to the physical phenomena observed during measurements. The main steps in this analysis can be seen represented on Fig. 6.
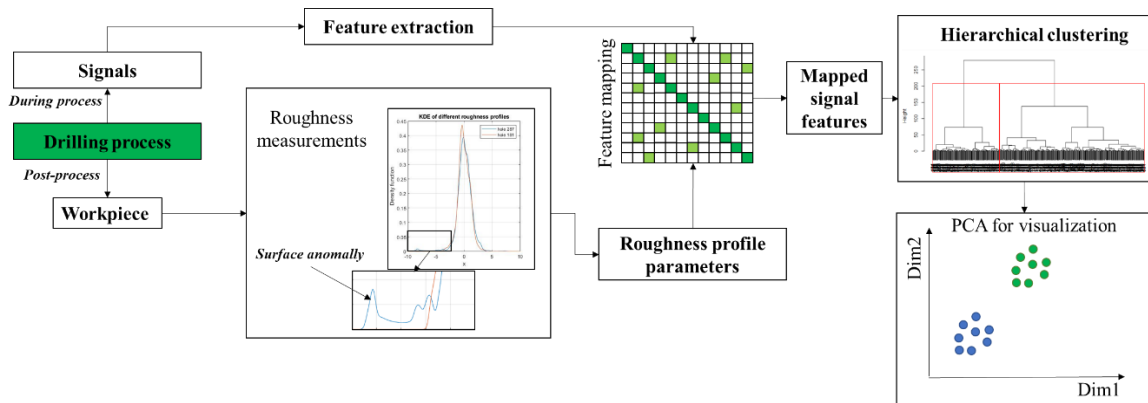

Fig 6 Statistical feature selection of external and internal signals for hole surface anomaly detection

Roughness parameters with linear relations are removed (those having a coefficient above 99%). After that, only statistical features of the acquired signals with correlation coefficient above 90% to these roughness parameters are selected.

To evaluate the suitability of these statistical features for the automatic identification of workpiece contact properties, hierarchical clustering is carried out: (i) first only considering the selected surface roughness parameters and then, (ii) only considering the statistical features that belong to the roughness measured holes and which are correlated with the roughness parameters used in the previous step. Finally, the similarity between the dendrograms created on both steps are compared.

For the creation of the bottom-up dendrograms in hierarchical clustering, both when using roughness parameters and when using clustering with features extracted from internal signals and/or sensors, the Euclidean distance was used between points/observations and the Ward's minimum variance method for linkage purposes, in which the fusion of two clusters is based on the size of an error sum-of-squares criterion. The AHC algorithm used corresponds to the implementation of the command "hclust" that can be found in the R programming language library named "stats".

Using the clusters generated, the rest of the holes are projected on these clusters using PCA to see if they are representative of the extended population of holes.

3   Results and discussion

3.1   Roughness parameters selection and clustering

To classify the deviation on the machined surface roughness profiles, hierarchical clustering was used, using initially 6 measured holes for each of the tools. The clusters were created from the roughness parameter data obtained from the measurements in the Alicona system after the tests. As many of these parameters were highly related, those variables that are highly correlated were removed. Then, parameters have been normalised so that they have an average equal to 0 and standard deviation 1 ($\mu=0$, $\sigma=1$).

Starting from 13 roughness variables *Ra, Rp, Rv, Rsm, Rsk, Rku, Rdq Rq, Rt, Rz, Rmax, Rc, Rt/Rz*, 4 variables were identified that are not correlated with the rest *Ra, Rp, Rsk, Rdq* nor between them, and common to both tools. and 3 specific to each tool, neither correlated with the rest nor between them, therefore clustering process uses 7 parameters for each tool, as it can be seen in Table 3.

Specifically, for the holes made with R204.6D, the parameters *Rt, Rmax, Rt/Rz, Rz, Rc, Rq* have been neglected and not taken into account in the analysis. For the holes made with the BH04.5D tool, *Rt, Rmax, Rt/Rz, Rp, Rv, Rku* are the parameters that were neglected. Cutting the dendrogram to create two clusters, identified holes 196 and 287 as distinct from the rest of the holes for tools R204.6D and BH04.5D respectively. Table 3 shows the dendrograms for the measured holes corresponding to each tool.

Table 3 *Uncorrelated surface parameters and their respective dendrograms for both tools*

Common parameters	*Ra, Rp, Rsk, Rdq*	
Tool specific parameters	*Rku, Rv, Rsm*	*Rc, Rq, Rz*
Dendrogram	Dendrogram of R204.6D tool	Dendrogram of BH04.5D tool

The y-axis shows how similar the observations or groups of observations are. Each connection of two groups is represented in the graph by dividing a vertical line into two vertical lines. The vertical position of the division, shown by the horizontal bar, gives the distance (dissimilarity) between two groups. As shown in Table 3, holes 196 and 287 are remarkably different from the rest of the observations for tools R204.6D and BH04.5D, respectively.

In figure 7, after clustering, the 6 observations are shown according to sample number and roughness parameters coloured according to the cluster they belong to and labelled with the corresponding hole number. Each observation represents the average of the two measurements made on each of the holes.
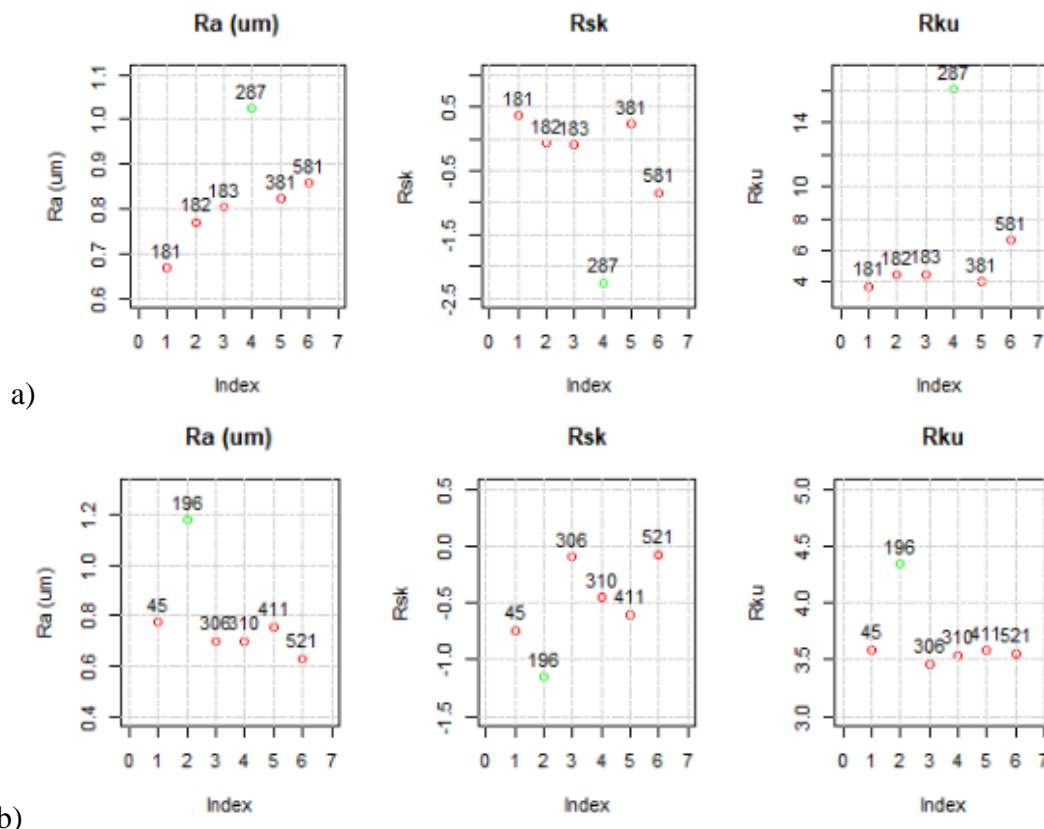

Fig 1 Analysing roughness parameters individually through clustering results a) BH04.5D b) R204.6D

For every hole made with each of the tools, two types of surface profiles have been observed. On the one hand, in hole 287, made with tool BH04.5D, there were marks that did not correspond to the tool feed rate (surface tearing) and holes with no visible damage have been

observed. In hole 196, made with the tool R204.6D, deep feed marks were seen compared to the rest of the holes. These observed phenomena caused the roughness to be affected at certain points of the process.

Discarding the damaged surface values (hole 196 for R204.6D and hole 287 for BH04.5D) the average *Ra* values are 0.71 μm and 0.78 μm for R204.6D and BH04.5D tools respectively showing a negligible increase in roughness mean value.

3.2 Signal statistical feature selection and clustering of measured holes

For selecting the most representative signals regarding roughness, correlation analysis has been carried out with respect to the filtered roughness parameters among all the statistical features obtained from the signals. Statistical features with correlations to roughness measures above 90% are selected and neglected below 90%. Table 6 shows features with a high correlation coefficient with one or more roughness parameters.
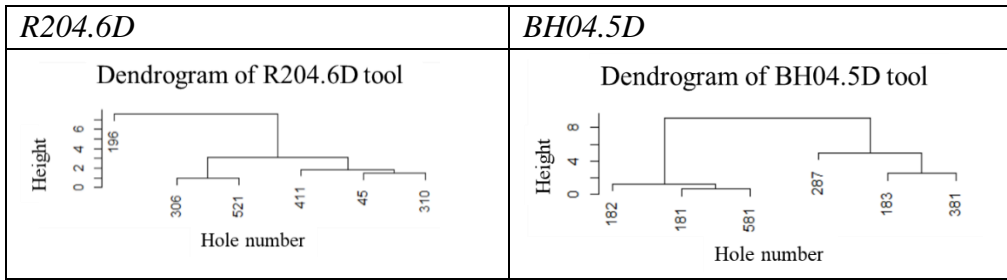
Table 4 *Correlations higher than 90% between acquired signal statistical features and roughness measured parameters. Blank cells are those with a correlation of over 90%, while shaded cells are those with a correlation of less than 90%. a) R204.6D tool measured holes b) BH04.5D tool measured holes*

a) R204.6D	Ra	Rp	Rv	Rsm	Rsk	Rku	Rdq
Fy_skew	0.81	0.45	0.84	0.91	-0.89	0.82	0.21
ACCx1_min	-0.89	-0.75	-0.86	-0.81	0.78	-0.92	-0.56
ACCx1_kurt	0.94	0.76	0.91	0.79	-0.78	0.96	0.68
ACCy2_skew	0.93	0.68	0.92	0.79	-0.77	0.97	0.7
AE_kurt	0.93	0.67	0.91	0.81	-0.77	0.88	0.61
TV2_max	0.63	0.96	0.48	0.40	-0.24	0.67	0.81
TV3_min	0.82	0.31	0.89	0.96	-0.98	0.71	0.04
b) BH04.5D	Ra	Rq	Rz	Rp	Rc	Rsk	Rdq
Mz_mean	0.03	-0.11	0.14	0.20	-0.01	0.33	0.91
ACCy_max	0.06	-0.04	0.24	0.32	0.08	0.26	0.97
ACCx2_mean	-0.76	-0.76	-0.82	-0.93	-0.81	-0.62	-0.55
ACCx2_rms	-0.82	-0.86	-0.81	-0.94	-0.87	0.75	-0.33
ACCz2_rms	-0.84	-0.93	-0.81	-0.81	-0.90	0.96	0.08
ACCz2_min	0.75	0.84	0.71	0.62	0.81	-0.93	-0.26
TV50_mean	0.23	0.11	0.34	0.43	0.21	0.12	0.96
TV50_max	0.21	0.09	0.32	0.43	0.19	0.13	0.95

Both, the roughness parameters and the statistical features of the acquired signals are filtered differently for each tool, as the phenomena observed in the roughness profiles are also different. In the holes made with the R204.6D tool, more visible feed marks are seen (Fig 4), which causes the roughness to increase, having a negative impact on the profile skewness value. In the worst case scenario measured with the BH04.5D tool (hole 287), surface tearing can be seen, which highly increases the *Ra* value.

In a next step, the statistical features of the signals shown in Table 4 were the inputs for another hierarchical clustering to compare the similarities shown by these statistical features and those obtained from the roughness parameters in Table 3. Table 5 shows the dendrograms obtained as a result of this process.

Table 5 *Clustering of measured holes using the signal statistical features of signals shown in Table 4*

R204.6D	BH04.5D

3.3 Hierarchical clustering in a bigger observation space

Following with the proposed methodology, hierarchical clustering has been applied to the entire set of observations made for each of the tools using the signal statistical features during the selection of variables, to see how accurately the selected signals can predict the differences between the profile distributions. Fig. 8 shows the dendrograms obtained for the holes made with each of the tools, in the dendrograms two groups can be seen clearly.
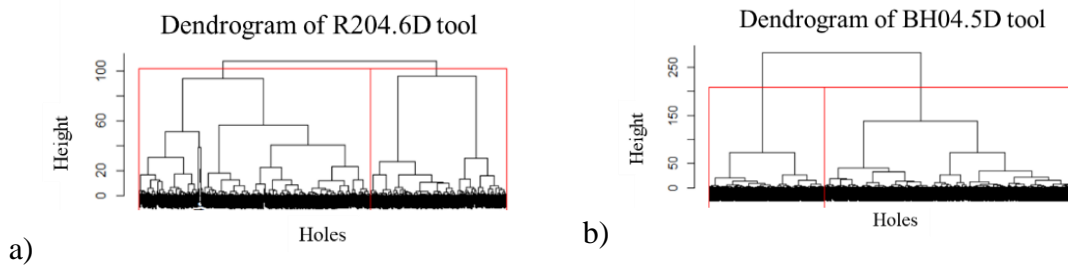

Fig 7 Dendrograms using the statistical features of all the holes for each of the cutting tools used

During the assignment of the clusters, the *Si* (silhouette coefficient) of each one of the observations has been evaluated. The silhouette coefficient (*Si*) measures how similar an object *i* is to the other objects in its own cluster compared to those in the neighbouring cluster. Those observations with a silhouette coefficient below 0 have been taken to the nearest neighbour; this operation is carried out recursively until all the observations assigned to a given cluster have a *Si* higher than 0.

3.4 Visualisation of obtained clusters and evaluation of the principal components of the clusters

For the display of the clusters, the principal component analysis (PCA) was used. Fig. 9 shows the two main components for the holes made with each of the tools. The colours show each of the clusters. More information on the PCA can be found in Annex A.2.
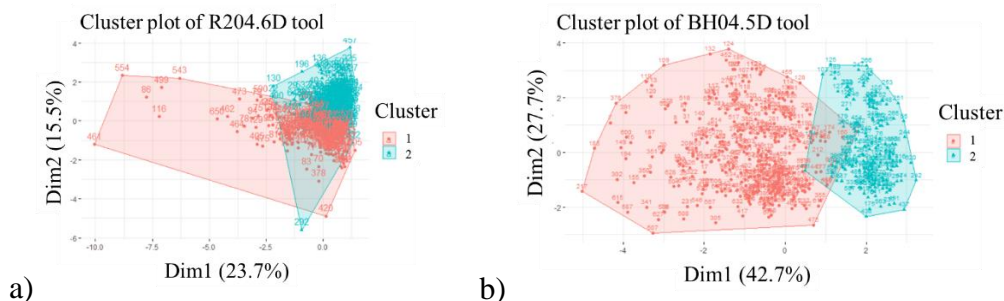

Fig 8 Visualisation of two principal components for obtained clusters a) R204.6D tool b) BH04.5D tool

According to the dendrogram for tool R204.6D in Fig 9 a), groups 1 and 2 are closer to each other while for BH04.5D tool, the clusters are well separated.

14

For tool R204.6D, holes 45, 196, 411 belongs to cluster 2 while holes 306, 310, and 521 belongs to cluster 1. Holes 45 and 411 that was supposed to be in cluster 1 fall in cluster 2, the holes are in the boundary of the two clusters, so they are more confusing, this is discussed below in Fig 13. Regarding tool BH04.5D hole 287 belong to group 1 (green), the rest of the measured holes belongs to group 2.

To find out which variables have the most significant variability in each of the dimensions, the percentage of the variance of each of the dimensions obtained in the principal component analysis and the contribution of each of the variables in the two principal components have been obtained. This can be seen in Fig 10.
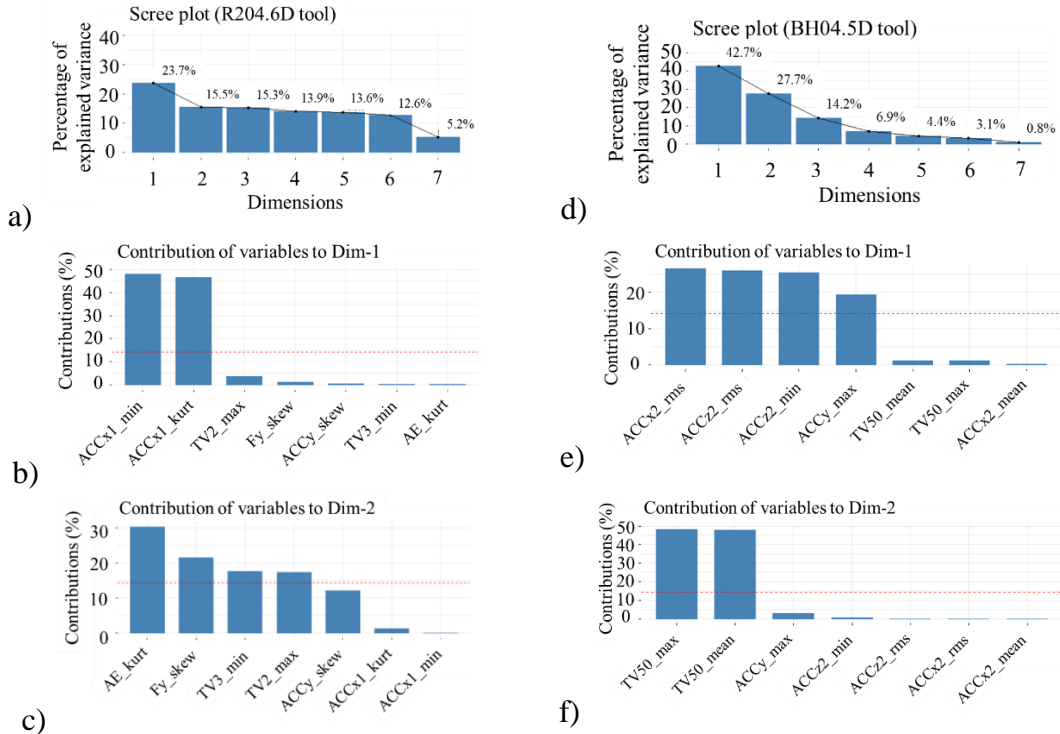

Fig 9 *Principal component analysis a) Percentage of explained variance for R204.6D tool b) Contribution of each statistical feature to Dim1 of R204.6D tool c) Contribution of each statistical feature to Dim2 of R204.6D tool d)Percentage of explained variance for BH04.5D tool e) Contribution of each statistical feature to Dim1 of BH04.5D tool f) Contribution of each statistical feature to Dim2 of BH04.5D tool*

In the holes made with the R204.6D tool, in the first dimension, the kurtosis value of the vibrations in the X-axis at low frequencies (ACCx1_kurt) and the minimum of the same signal (ACCx1_min) are the ones that have the greatest contribution. In the second dimension TV2_max, TV3_min, AE_kurt and Fy_skew are the ones that have the most significant contribution.

The holes made with the BH04.5D tool, the statistical features ACCx2_rms, ACCz2_rms, ACCz2_min and ACCy_max are the ones that contribute most to the first dimension. In this tool the vibration signals are more affected by what happens on the surface of the working material. In the second dimension, TV51_max and TV51_mean have an equal contribution. The ACCx2_mean feature has a null contribution; this was expected since the centre of the vibration signal is around 0, so this feature could be removed to reduce the feature space.

In table 6 the centroids of each of the clusters can be seen for R204.6D tool. The centroids are the mean value of each of the variables for each of the clusters and explain the effect that the roughness has suffered on that particular variable. The contributions of each of the variables to dimensions 1 and 2 of the principal component analysis can also be seen in the table.

Table 6 *Cluster centroids for R204.6D tool drilled holes and feature contribution to each dimension*

Cluster	Holes	Dim2 Fy_skew (15%)	Dim1 ACCx1_min (49%)	Dim1 ACCx1_kurt (49%)	ACCy2_skew (-)	Dim2 AE_kurt (21%)	Dim2 TV2_max (34%)	Dim2 TV3_min (24%)
1	45,196,411	-0.158	-0.172	0.169	-0.030	-0.296	-0.199	-0.400
2	306,310,521	0.269	0.293	-0.288	0.051	0.505	0.339	0.682

The same procedure can be seen in table 7 for tool BH04.5D.

Table 7 *Cluster centroids for BH04.5D tool drilled holes and feature contribution to each dimension*

Cluster	Holes	Dim1 ACCy_max (19%)	ACCx2_mean (-)	Dim1 ACCx2_rms (37%)	Dim1 ACCz2_rms (36%)	Dim1 ACCz2_min (35%)	Dim2 TV50_mean (49%)	Dim2 TV50_max (49%)
1	183,381,181, 182,581	0.376	-0.027	0.550	0.509	-0.433	0.051	0.065
2	287	-0.818	0.06	-1.198	-1.109	0.943	-0.112	-0.141

To analyse the compactness of each of the clusters, the intra-cluster distance has been measured. For this purpose, the mean of the distances from the observations to the centroid of their cluster is calculated. Besides, the distances of the holes considered for measurement to the centre of the clusters have been measured. This information can be seen in tables 8 and 9. The numbers in bold are the distances to the clusters to which each hole belongs.

Table 8 *Intra cluster distance and distance between measured holes and cluster centroids R204.6D tool*

Cluster	Intra cluster distance	Distance between measured holes and cluster centroids					
		Hole 45	Hole 196	Hole 306	Hole 310	Hole 411	Hole 521
1	2.14	2.069	3.426	**1.576**	**1.448**	1.844	**1.157**
2	2.57	**1.588**	**2.533**	1.773	1.871	**1.345**	1.713

In the case of tool R204.6D, holes 45 and 411 belong to cluster 2, and are located at the boundary of the clusters, as shown in Fig 13 a). These were expected to be in cluster 1, and as they are located in a boundary region between two clusters the correct assignment is more complicated.

Table 9 *Intra cluster distance and distance between measured holes and cluster centroids BH04.5D tool*

Cluster	Intra cluster distance	Distance between measured holes and cluster centroids					
		Hole 181	Hole 182	Hole 183	Hole 287	Hole 381	Hole 581
1	2.252	**2.268**	**2.224**	**1.206**	3.226	**2.221**	**2.417**
2	3.499	3.355	2.982	3.360	**1.430**	4.109	3.067

Concerning the BH04.5D tool, cluster 1 is the most compact and cluster 2 show an increase in the mean values of the distances of their corresponding observations. The randomly selected holes for this tool apparently, are more central to their cluster centroids.

3.5 *Validation of obtained clusters*

To validate the obtained clusters, a new branch of holes has been selected again to validate the process.

The clusters obtained for the BH04.5D tool are shown in Fig. 11. In this case, all the holes measured for the validation correspond to their respective clusters. Fig 11 a) shows the clusters in the first two main components of the signal features considered for creating the clusters. Fig 11 b) shows the dendrogram of the roughness parameters obtained from the profiles measured

in Alicona. The mapping made between the statistical features of the signals and the measured holes matches 100% of the total measured holes.

a)   b)
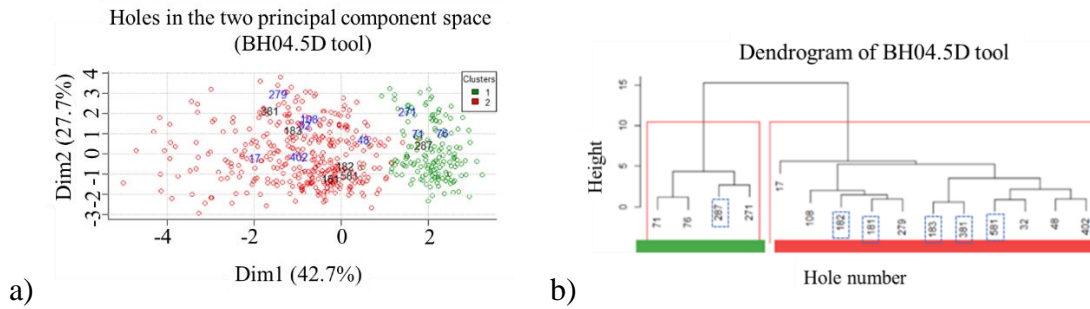
Fig 10 Validation data for BH04.5D (straight edge) tool, a) Obtained clusters from sensor data in two principal component space of the selected features, labels in black are the holes used for the cluster creation, labels in blue are the holes measured after the clusters were created b) Obtained clusters from surface measurement data (green and red colours express the clusters of the figure a).

Equations 1 and 2 show the linear combinations of the two principal components used to display the obtained clusters in Fig 11 a).

The equations obtained from the principal component analysis are used to translate a hole into the 2 dimensions presented in Fig 11 a). Having the following normalised features for hole 271; ACCx2_rms=-1.372, ACCz2_rms=-0.279, ACCz2_min=1.007, ACCy_max=-0.898, TV50_max=0.846, TV50_mean=0.998, and using these values and equations 1 and 2 this point can be projected in the new space substituting the values in both equations, obtaining a point with the following values, Dim1=1.74 and Dim2=1.27. A new hole made under the same conditions can be quickly located on the map following the same procedure.

$$Dim1 = -0.51 \cdot ACCx2_{rms} - 0.51 \cdot ACCz2_{rms} + 0.5 \cdot ACCz2_{min} - 0.44 \cdot ACC_{ymax} \qquad [1]$$

$$Dim2 = 0.69 \cdot TV50_{max} + 0.69 \cdot TV50_{mean} \qquad [2]$$

To establish the space covered by the selection of the statistical features, the corresponding area to the two principal components $A = 55.45$ and the area corresponding to the holes measured for the creation of the clusters $A(181,182,183,287,381,581) = 11.82$ has been calculated. Overall, 21% of the area has been covered and the distance between two clusters, that is, the inter-cluster distance is 3.014. Fig. 12 shows the measured surfaces and their corresponding roughness profiles. Fig 12 a) shows a surface where some kind of error has been observed, in this case, surface tearing. Fig 12 b) shows a surfaces that is free of visible defects.
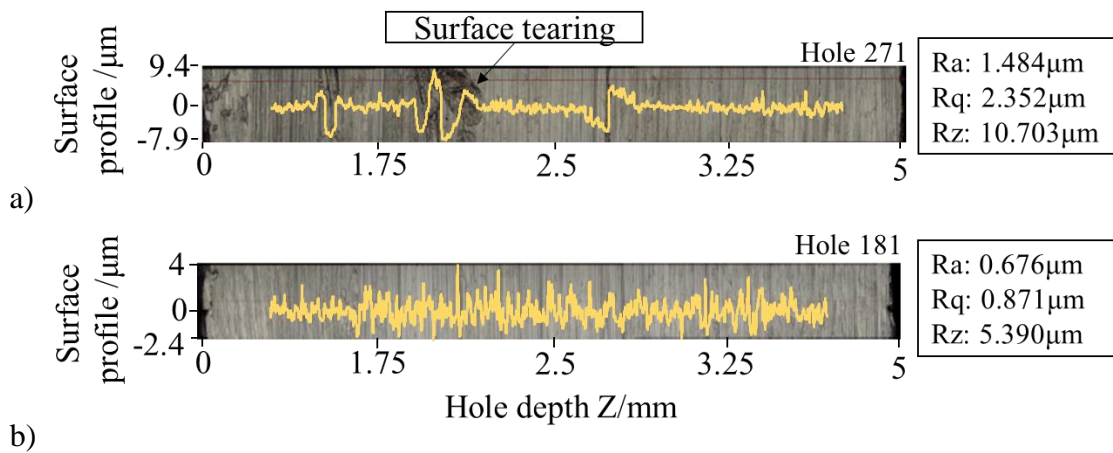

a)

b)

Fig 11 Hole surfaces and surface profiles obtained with BH04.5D tool a) Observed surface tearing b) Free damage surface

With respect to tool R204.6D, Fig 13 a) shows the clusters from the features of the acquired signals and the boundary between the two clusters. Fig 13 b) shows the dendrogram made with the roughness parameters obtained from the profiles.
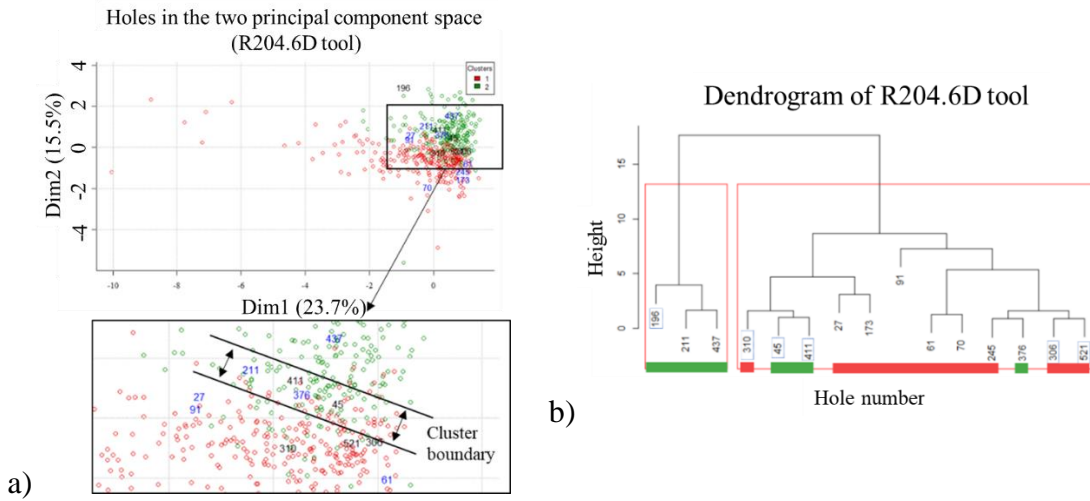

Fig 12 *Validation data for R204.6D (curved edge) tool, a) Obtained clusters from sensor data in two principal component space of the selected features and holes in clusters boundaries b) Obtained clusters from surface measurement data. Red colour corresponds to cluster 1 and green colour to cluster 2.*

The dendrogram shows that holes 45, 411 and 376 (marked in green) belongs to cluster 2 although they were expected to be in cluster 1. In the zoom made in Fig 13 a) it can be observed that these holes belong to the cluster boundary.

Equations 3 and 4 show the linear combinations of the two principal components used to display the obtained clusters in Fig 14 a).

$$Dim1 = 0.69 \cdot ACCx1_{min} - 0.68 \cdot ACCx1_{kurt} \qquad [3]$$

$$Dim2 = 0.55 \cdot AE_{kurt} + 0.46 \cdot Fy_{skew} + 0.41 \cdot TV3_{min} + 0.41 \cdot TV2_{max} + 0.34 \cdot ACCy2_{skew} \qquad [4]$$

The area corresponding to the two principal components is $A = 107.45$ and the area corresponding to the holes measured for the creation of the clusters is $A(45,196,306,310,411,521) = 6.02$. Therefore, 5.6% of the area has been covered. The inter-cluster distance is 1.65. Fig. 14 shows the measured surfaces and their corresponding roughness profiles. Fig 14 a) more visible feed marks can be seen whereas in Fig 14 b) a lower surface roughness is seen with no visible feed marks. These feed marks do not show a trend in terms of the time series in which the holes have been made and could be due to other factors such as a built-up edge on the periphery of the tool.
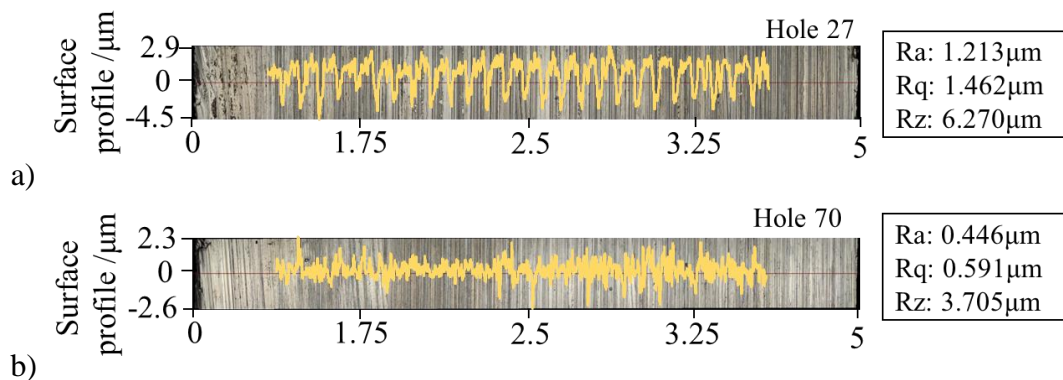

Fig 13 *Hole surfaces and surface profiles obtained with R204.6D tool a) Observed feed marks b) Free of feed marks*

In the BH04.5D tool, the area covered by the measured holes is more extensive than in the R204.6D tool, and better result is obtained, achieving a better separation between the clusters.

The creation of a supervised learning system requires the measurement of a large number of observations. The feasibility of this depends on the resources and time available. Obtaining classification models of roughness, in case of not having internal or external signals or only having process parameters is a complex task. Several parameters influence the roughness of a component and influence the signals that can be collected during an operation. In this work, we show a methodology that can create descriptors of the roughness obtained by measuring a small sample of the set of observations to be evaluated. Although it is not an exact value of roughness, the descriptors are based on different parameters of the measured profile to create a model capable of classifying each of the holes made without the need for physical measurement. As in the work done by Kubišová et al. [36] the use of hierarchical clustering is highly valued to obtain information about the replicability of surfaces under specific cutting conditions.

The area covered by the holes measured on the map of the principal components plays an essential role in the methodology developed. It was found that with the R204.6D tool some of the holes were in the cluster boundary, while with the BH04.5D tool all the holes measured, both prior and for the validation, were identified in 100% of the measured cases on each respective cluster. The former presents less amplification in the roughness parameters measured in the laboratory in those holes classified as faulty, while the latter presents roughness parameters amplified to almost twice.

There is no direct effect on the features of a given signal directly related to the roughness profile of a component. As can be the case with tool wear, which has been shown that the increase in thrust force in drilling processes is very closely related to the tool wear curve [37]. Although many works show an increase in roughness values as well as tool wear, some temporal event in the middle of the process may cause the surface of the component to be damaged or the roughness value to increase during the same tool condition. This study shows that with two different cutting tools blocking the cutting conditions, surface roughness variations can be seen without tool wear.

The works consulted to date only contemplate the parameter *Ra* for monitoring the roughness of a given component [38,39], as seen in Djebala et al. [40] other roughness parameters can describe the fatigue or assembly properties. The *Rsk* value of a roughness profile can be of great importance; thus, an excessively negative skewness could lead to early fracture occurrence. However, it can be beneficial for assembly. Conversely, a positive skewness can lead to assembly problems and be beneficial for components where long useful life is expected. Therefore, the system proposed in this work has the benefit of using several roughness profile parameters. This leads to a better interpretation of the surface property characteristics of a component depending on the sector for which it is being manufactured.

The chip is fan-shaped on the R204.6D tool, which occurs when the chip is broken before a complete revolution; this is the ideal chip in drilling processes and the one that is best evacuated [41]. On the BH04.5D tool, the chip is somewhat longer and is a mixture of fan-shaped and conical, presenting a higher difficulty in the evacuation, and therefore could lead to surface tearing on the machined surface.

The feed marks shown on the hole surface profile from R204.6D tool which makes roughness mean value to increase with this specific tool can be regarded to wedge angle of 55° which is a narrower angle than the BH04.5D tool. Conversely, on tool BH04.5D, with a wedge angle of 80° and a more positive rake angle can facilitate the chip rubbing against the generated surface, and thus, to surface tearing appearing.

The surface tearing observed in the holes made with tool BH04.5D (straight edge) could be due to chip clogging. The phenomenon has been observed in the first half of the hole in all cases (Z< 2.5 mm), which suggests that it is the part of the surface that experiences the most damage during drilling.

Concerning the descriptors (categories) created, it is possible that for each of the tools used in other cutting conditions, there are other possible phenomena not visualised in the measurements made under the cutting conditions used. Tool wear, which is not analysed in this study, could also lead to the appearance of other types of defects that cause the machined surface to be negatively affected. So it is of interest to analyse the phenomena that may appear to decrease the limitations of this system. The statistical features related to the roughness profiles shown could change. Thus, a study of different cutting conditions and different tool conditions that increase the space of variables used and, consequently, creating a greater number of clusters is of interest.

4   Conclusions and future work

In this work, hierarchical clustering of holes is made with two different tools to describe the surface roughness obtained. For the characterisation of the roughness of the machined components, several surface profile parameters measured in the Alicona profilometer were used. Once the statistical features of the signals collected during the drilling of holes have been identified, clustering is carried out for 600 holes. The major contribution of this work results in the development of a new methodology capable of giving a descriptor of the quality of the surface generated in drilling processes based on the least number of measurements possible through the use of hierarchical clustering and internal and external signals to the cutting process. The result is a virtual metrology system for a more extensive set of holes than those physically measured. The following are the main conclusions:

- There was no tool wear identified during the tests. However, there was a variation in roughness. Events that occur at specific points in the cutting process cause the surface profile of the machined component to be affected. Therefore, in certain processes tool wear is not directly related to surface roughness. However, end-of-life tests should be carried out to evaluate the relationship between wear and surface roughness.
- The events or phenomena observed on the machined surface that appear using two tool geometries are different. Consequently, the signals used to characterise the roughness result to be different, avoiding the use of the same variables to characterise the surface generated in the drilling processes.
- Clustering algorithms used with signals can approximate the roughness obtained and perform a classification of the holes without the need to measure a large number of them. In this way, a roughness estimation can be obtained by measuring just a few holes and projecting them in the signal space.
- The area covered with the measurements on the data observation space is of great relevance for a good mapping of the roughness parameters using the data gathered during the process. As can be seen with the R204.6D tool, not all the erroneous holes have been identified in their respective clusters, while with the BH04.5D tool, 100% have been identified.
- Each of the two tools used generates a surface with different contact properties. Tool R204.6D shows feed marks per revolution on surfaces where the mean value of the roughness profile is increased. In contrast, tool BH04.5D shows surface tearing on surfaces where the Ra value is increased. Besides, tool R204.6D generates lower thrust force than BH04.5D tool due to smaller rake angle. The amplification of the roughness

parameters of the individual tools influences the signal features, which makes it possible to identify the differences in the changes of the roughness profile distribution.

- Further research will focus on employing one-class classifiers. This would help to discriminate those surface distributions that present deviations from the contact properties expected to be achieved in a specific process.

References

[1]   A. Duo, R. Basagoiti, P.J. Arrazola, J. Aperribay, M. Cuesta, The capacity of statistical features extracted from multiple signals to predict tool wear in the drilling process, International Journal of Advanced Manufacturing Technology. (2019) 5–8. https://doi.org/10.1007/s00170-019-03300-5.

[2]   A. Caggiano, Tool wear prediction in Ti-6Al-4V machining through multiple sensor monitoring and PCA features pattern recognition, Sensors (Switzerland). 18 (2018). https://doi.org/10.3390/s18030823.

[3]   J.C. Jauregui, J.R. Resendiz, S. Thenozhi, T. Szalay, A. Jacso, M. Takacs, Frequency and Time-Frequency Analysis of Cutting Force and Vibration Signals for Tool Condition Monitoring, IEEE Access. 6 (2018) 6400–6410. https://doi.org/10.1109/ACCESS.2018.2797003.

[4]   D. D'Addona, T. Segreto, A. Simeone, R. Teti, ANN tool wear modelling in the machining of nickel superalloy industrial products, CIRP Journal of Manufacturing Science and Technology. 4 (2011) 33–37. https://doi.org/10.1016/j.cirpj.2011.07.003.

[5]   C. Leone, D.D. Addona, R. Teti, Tool wear modelling through regression analysis and intelligent methods for nickel base alloy machining, CIRP Journal of Manufacturing Science and Technology. 4 (2011) 327–331. https://doi.org/10.1016/j.cirpj.2011.03.009.

[6]   K. Subramanian, N.H. Cook, Sensing of Drill Wear and Prediction of Drill Life, The ASME International Mechanical Engineering Congress and Exhibition, OrlandoHE AMERICAN SOCIETY OF MECHANICAL ENGINEER. 65 (1977) 854. https://doi.org/10.1016/j.crad.2010.04.020.

[7]   L.H. Saw, L.W. Ho, M.C. Yew, F. Yusof, N.A. Pambudi, T.C. Ng, M.K. Yew, Sensitivity analysis of drill wear and optimization using Adaptive Neuro fuzzy-genetic algorithm technique toward sustainable machining, Journal of Cleaner Production. 172 (2018) 3289–3298. https://doi.org/10.1016/j.jclepro.2017.10.303.

[8]   A. Kumar, J. Ramkumar, N.K. Verma, S. Dixit, Detection and classification for faults in drilling process using vibration analysis, 2014 International Conference on Prognostics and Health Management, PHM 2014. (2015) 3–8. https://doi.org/10.1109/ICPHM.2014.7036393.

[9]   S.L. Chen, C.F. Su, Y.T. Cheng, A novel framework for diagnosing automatic tool changer and tool life based on cloud computing, Advances in Mechanical Engineering. 8 (2016) 1–12. https://doi.org/10.1177/1687814016637319.

[10]   R. Heinemann, S. Hinduja, A new strategy for tool condition monitoring of small diameter twist drills in deep-hole drilling, International Journal of Machine Tools and Manufacture. 52 (2012) 69–76. https://doi.org/10.1016/j.ijmachtools.2011.09.002.

[11]   G. Ferrari, M.P. Gómez, Correlation Between Acoustic Emission, Thrust and Tool Wear in Drilling, Procedia Materials Science. 8 (2015) 693–701. https://doi.org/10.1002/ejhf.1115.

[12]   L.A. Franco-Gasca, G. Herrera-Ruiz, R. Peniche-Vera, R.D.J. Romero-Troncoso, W. Leal-Tafolla, Sensorless tool failure monitoring system for drilling machines, International Journal of Machine Tools and Manufacture. 46 (2006) 381–386. https://doi.org/10.1016/j.ijmachtools.2005.05.012.

[13]   Y. Ao, G. Qiao, Prognostics for drilling process with wavelet packet decomposition, International Journal of Advanced Manufacturing Technology. 50 (2010) 47–52. https://doi.org/10.1007/s00170-009-2509-6.

[14]   A. Duo, R. Basagoiti, P.J. Arrazola, J. Aperribay, A comparative study between internal and external signals for tool wear detection in drilling processes, 14Th International Conference on High Speed Machining. (2018) 1–4.

[15]   P.G. Benardos, G.C. Vosniakos, Predicting surface roughness in machining: A review, International Journal of Machine Tools and Manufacture. 43 (2003) 833–844. https://doi.org/10.1016/S0890-6955(03)00059-2.

[16]   E.S. Gadelmawla, M.M. Koura, T.M.A. Maksoud, I.M. Elewa, H.H. Soliman, Roughness parameters, Journal of Materials Processing Technology. 123 (2002) 133–145. https://doi.org/10.1016/S0924-0136(02)00060-2.

[17]   ISO 4287-1997, Surface Texture Parameters, ASTM International. (1998) 1–65.

[18]   S. Zhang, W. Wang, Z. Zhao, The effect of surface roughness characteristics on the elastic-plastic contact performance, Tribology International. 79 (2014) 59–73. https://doi.org/10.1016/j.triboint.2014.05.016.

[19]   M.B.H. Amor, S. Belghith, S. Mezlini, H.B.H. Salah, Effect of skewness and roughness level on the mechanical behavior of a rough contact, Lecture Notes in Mechanical Engineering. 789 (2015) 377–386. https://doi.org/10.1007/978-3-319-17527-0_38.

[20]   E.S. Gadelmawla, M.M. Koura, T.M.A. Maksoud, I.M. Elewa, H.H. Soliman, Roughness parameters, Journal of Materials Processing Technology. 123 (2002) 133–145. https://doi.org/10.1016/S0924-0136(02)00060-2.

[21]   A. Thakur, S. Gangopadhyay, State-of-the-art in surface integrity in machining of nickel-based super alloys, International Journal of Machine Tools and Manufacture. 100 (2016) 25–54. https://doi.org/10.1016/j.ijmachtools.2015.10.001.

[22]   A. Yang, Y. Han, Y. Pan, H. Xing, J. Li, Optimum surface roughness prediction for titanium alloy by adopting response surface methodology, Results in Physics. (2017). https://doi.org/10.1016/j.rinp.2017.02.027.

[23] A. Thakur, S. Gangopadhyay, State-of-the-art in surface integrity in machining of nickel-based super alloys, International Journal of Machine Tools and Manufacture. 100 (2016) 25–54. https://doi.org/10.1016/j.ijmachtools.2015.10.001.

[24] E. García Plaza, P.J. Núñez López, Surface roughness monitoring by singular spectrum analysis of vibration signals, Mechanical Systems and Signal Processing. 84 (2017) 516–530. https://doi.org/10.1016/j.ymssp.2016.06.039.

[25] E. García Plaza, P.J. Núñez López, Analysis of cutting force signals by wavelet packet transform for surface roughness monitoring in CNC turning, Mechanical Systems and Signal Processing. 98 (2018) 634–651. https://doi.org/10.1016/j.ymssp.2017.05.006.

[26] E. García Plaza, P.J. Núñez López, E.M. Beamud González, Efficiency of vibration signal feature extraction for surface finish monitoring in CNC machining, Journal of Manufacturing Processes. 44 (2019) 145–157. https://doi.org/10.1016/j.jmapro.2019.05.046.

[27] S. Akincioğlu, F. Mendi, A. Çiçek, G. Akincioğlu, ANN-based prediction of surface and hole quality in drilling of AISI D2 cold work tool steel, International Journal of Advanced Manufacturing Technology. 68 (2013) 197–207. https://doi.org/10.1007/s00170-012-4719-6.

[28] O. Maimon, L. Rokach, Data mining and knowledge discovery handbook, 2011. https://doi.org/10.5860/choice.48-5729.

[29] B.S. Everitt, S. Landau, M. Leese, D. Stahl, Cluster analysis: Fifth edition, 2011. https://doi.org/10.1002/9780470977811.

[30] A. Duo, T. Segreto, A. Caggiano, R. Basagoiti, R. Teti, P.J. Arrazola, Drilling process monitoring: a framework for data gathering and feature, Procedia CIRP. 73 (2020) 86–90. https://doi.org/10.1016/j.procir.2021.03.123.

[31] S.A. Mingoti, J.O. Lima, Comparing SOM neural network with Fuzzy c-means, K-means and traditional hierarchical clustering algorithms, European Journal of Operational Research. 174 (2006) 1742–1759. https://doi.org/10.1016/j.ejor.2005.03.039.

[32] J. Diaz-Rozo, C. Bielza, P. Larrañaga, Machine Learning-based CPS for Clustering High throughput Machining Cycle Conditions, Procedia Manufacturing. 10 (2017) 997–1008. https://doi.org/10.1016/j.promfg.2017.07.091.

[33] L. Xiaoli, Y. Zhejun, Tool wear monitoring with wavelet packet transform - fuzzy clustering method, Wear. 219 (1998) 145–154.

[34] Z. Li, G. Wang, G. He, Milling tool wear state recognition based on partitioning around medoids (PAM) clustering, International Journal of Advanced Manufacturing Technology. 88 (2017) 1203–1213. https://doi.org/10.1007/s00170-016-8848-1.

[35] Y. Zhou, W. Yang, Z. Xu, X. Shi, Consistency evaluation of hole series surface quality using vibration signal, International Journal of Advanced Manufacturing Technology. 92 (2017) 1069–1079. https://doi.org/10.1007/s00170-017-0184-6.

[36] M. Kubišová, V. Pata, L. Sýkorová, M. Franková, Statistical Comparison of Original and Replicated Surfaces, 2019. https://doi.org/10.1007/978-3-030-18682-1_1.

[37] S.C. Lin, C.J. Ting, Tool wear monitoring in drilling using force signals, Wear. 180 (1995) 53–60. https://doi.org/10.1016/0043-1648(94)06539-X.

[38] Y. V. Deshpande, A.B. Andhare, P.M. Padole, Application of ANN to estimate surface roughness using cutting parameters, force, sound and vibration in turning of Inconel 718, SN Applied Sciences. 1 (2019). https://doi.org/10.1007/s42452-018-0098-4.

[39] M. Mia, N.R. Dhar, Prediction of surface roughness in hard turning under high pressure coolant using Artificial Neural Network, Measurement: Journal of the International Measurement Confederation. 92 (2016) 464–474. https://doi.org/10.1016/j.measurement.2016.06.048.

[40] A. Djebala, N. Ouelaa, M.K. Babouri, Design and Modeling of Mechanical Systems - II, 2015. https://doi.org/10.1007/978-3-319-17527-0.

[41] S.A. Batzer, D.M. Haan, P.D. Rao, W.W. Olson, J.W. Sutherland, Chip morphology and hole surface texture in the drilling of cast Aluminum alloys, Journal of Materials Processing Technology. 79 (1998) 72–78. https://doi.org/10.1016/S0924-0136(97)00324-5.